Modeling of screw feeder performance


Prabhu R Nott


Aashish Kumar Gupta

Indian Institute of Science
Bangalore

IFPRI funded project commenced on 21 October 2019

A brief history of screw conveyors/feeders

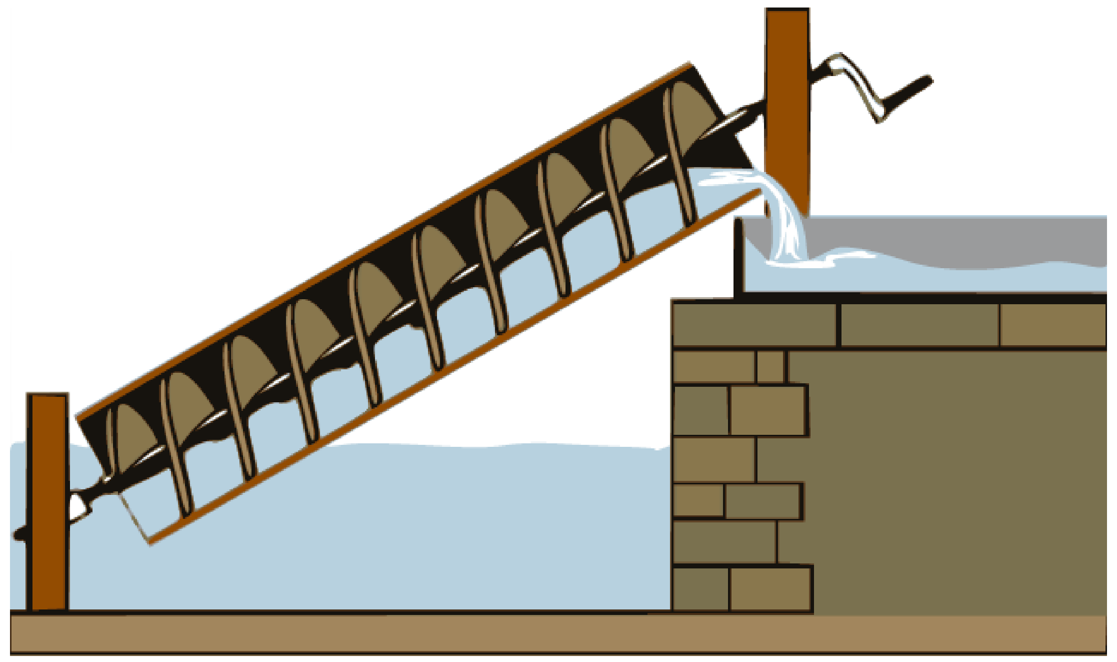

Dates back to ancient
Egypt (~ 3rd century BC)
for drawing water

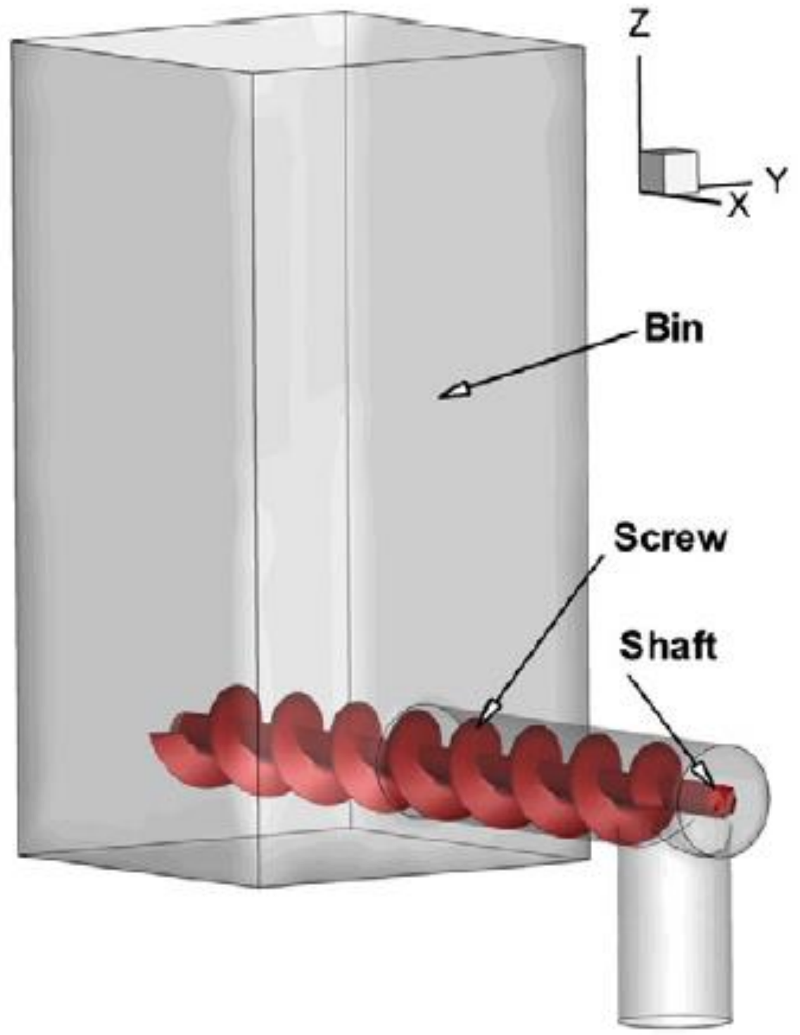

Remarkably, there is no analytical solution for even a Newtonian fluid!

Currently used widely for conveying of particulate materials in food, pharmaceutical, construction and mineral processing industries

Overview of the current work

- Develop of a simple mechanics-based model for the discharge rate through a screw feeder, under simple simplifying assumptions*.
- Understand the flow inside the feeder using simulations by the Discrete Element Method (DEM), and relax the simplifying assumptions.
- Study the stress variation on the surfaces of the feeder.

*Simplifying assumptions

- The space between the screw and the casing is completely filled with grains.
- Material inside the feeder moves as a plug.
- Gravity and centrifugal effects are neglected.

A simplistic analysis of the discharge rate

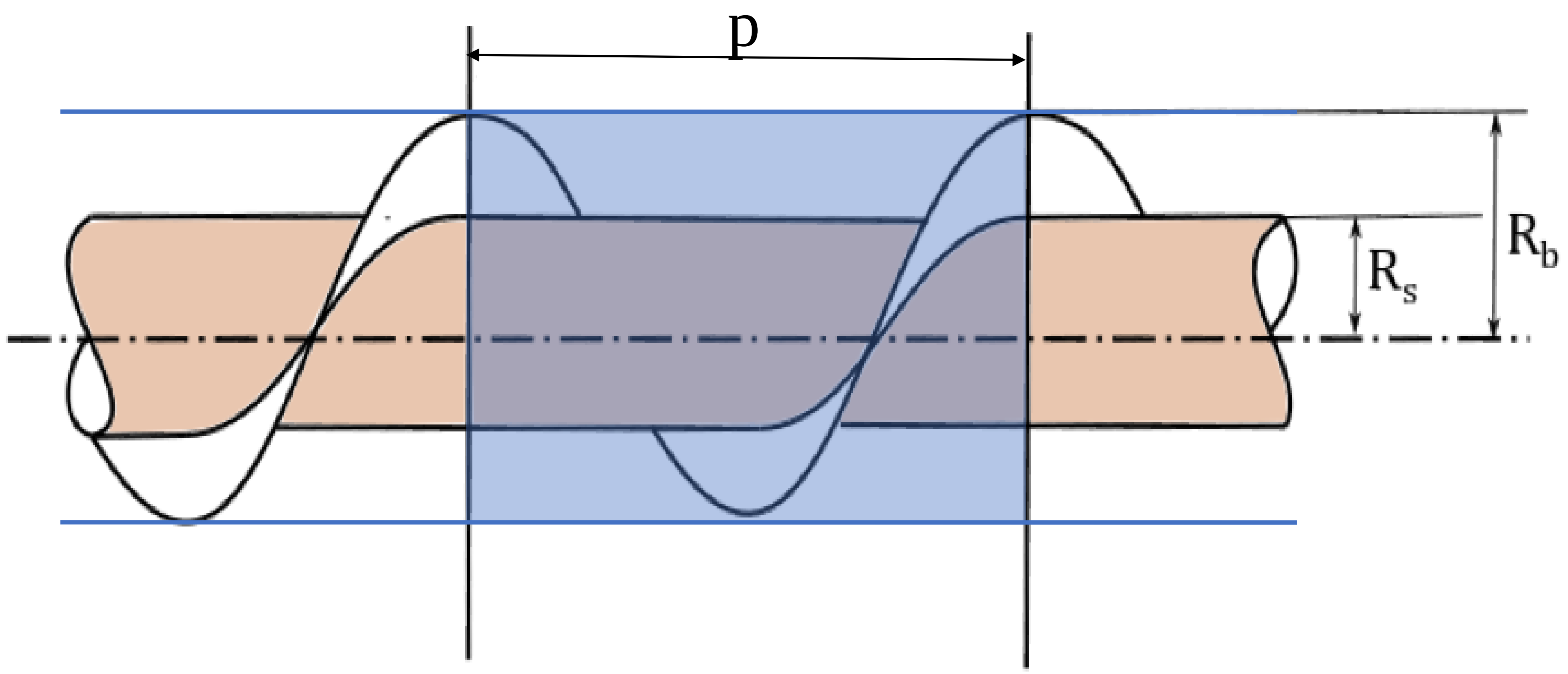

$$Q = \nu f \, \underline{p \, \pi (R_b^2 - R_s^2)}$$

ν : solids fraction
f : rotation frequency
p : screw pitch

Roberts, A. W., *Powder Technol.* **104**(1) (1999).

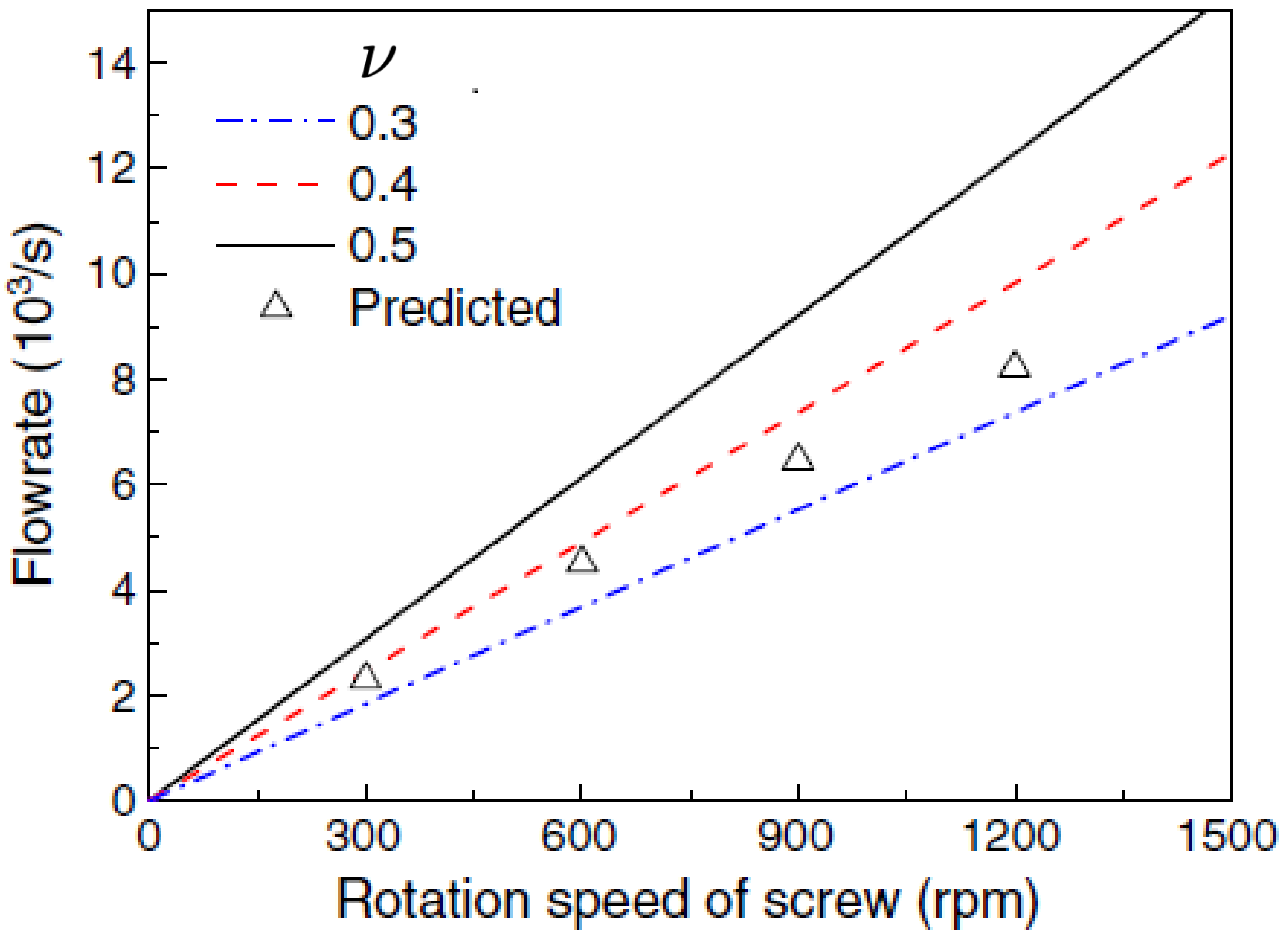

We will see that this a gross overestimate

Describing the screw surface

Screw surface: one parameter set of helices of pitch p

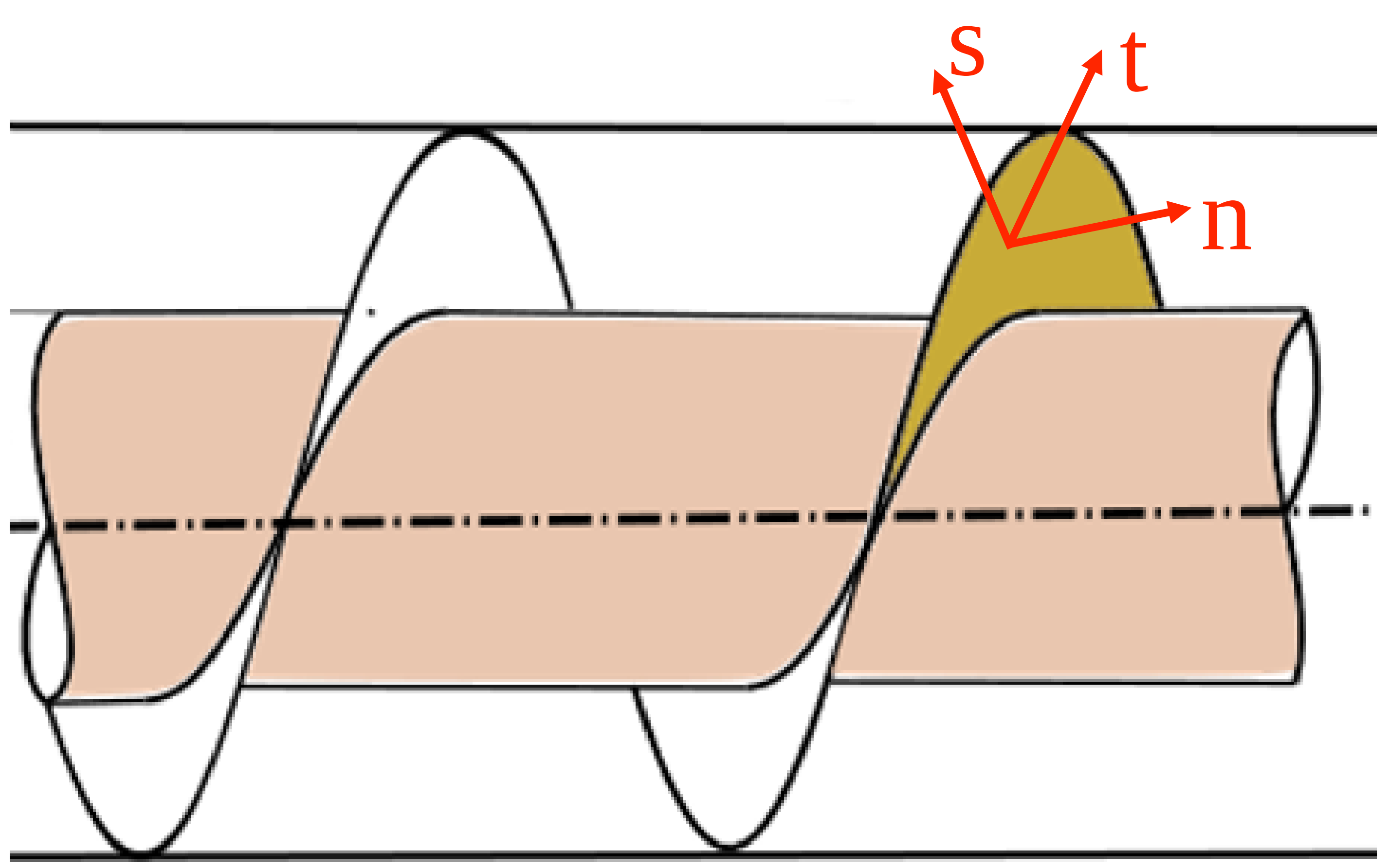

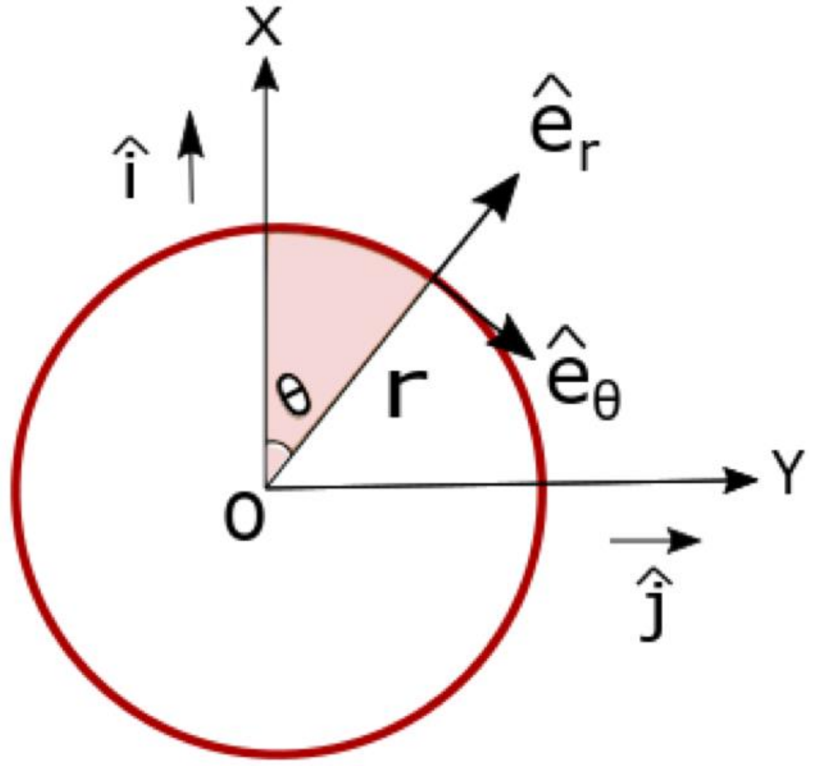

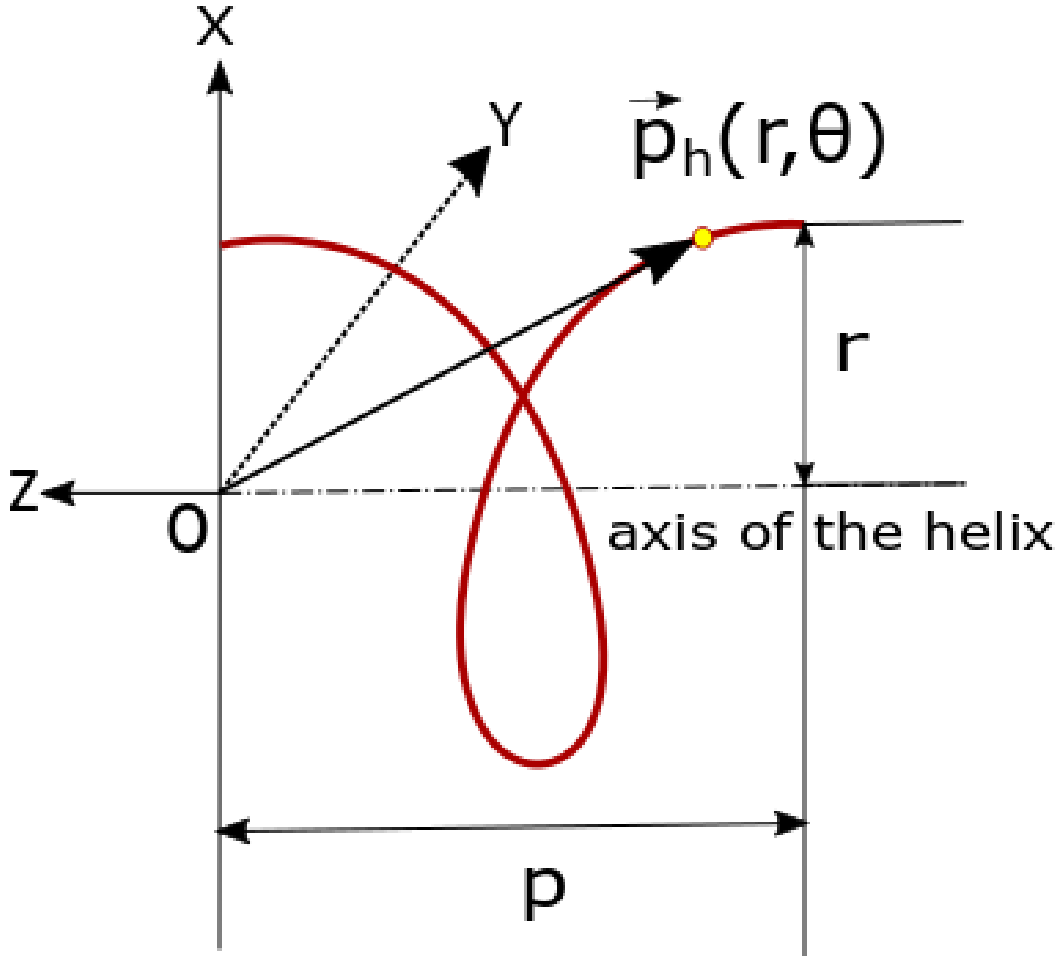

Equation of a helix: $\overrightarrow{P_h}(r,\theta) := (r\cos\theta)\hat{i} + (r\sin\theta)\hat{j} - \left(\frac{p\theta}{2\pi}\right)\hat{k}$

$$\hat{t}_h(r,\theta) = \left(\frac{\partial \overrightarrow{P_h}(r,\theta)}{\partial \theta}\right) \div \left|\frac{\partial \overrightarrow{P_h}(r,\theta)}{\partial \theta}\right| = \cos\alpha\ \hat{e}_\theta - \sin\alpha\ \hat{k}$$

$$\tan\alpha(r) = \frac{p}{2\pi r}$$

$$\hat{s}_h(r,\theta) = \left(\frac{\partial \overrightarrow{P_h}(r,\theta)}{\partial r}\right) \div \left|\frac{\partial \overrightarrow{P_h}(r,\theta)}{\partial r}\right| = \hat{e}_r$$

$$\hat{n}_h(r,\theta) = \hat{t}_h \times \hat{s}_h = -\sin\alpha\ \hat{e}_\theta - \cos\alpha\ \hat{e}_k$$

General expression for discharge rate

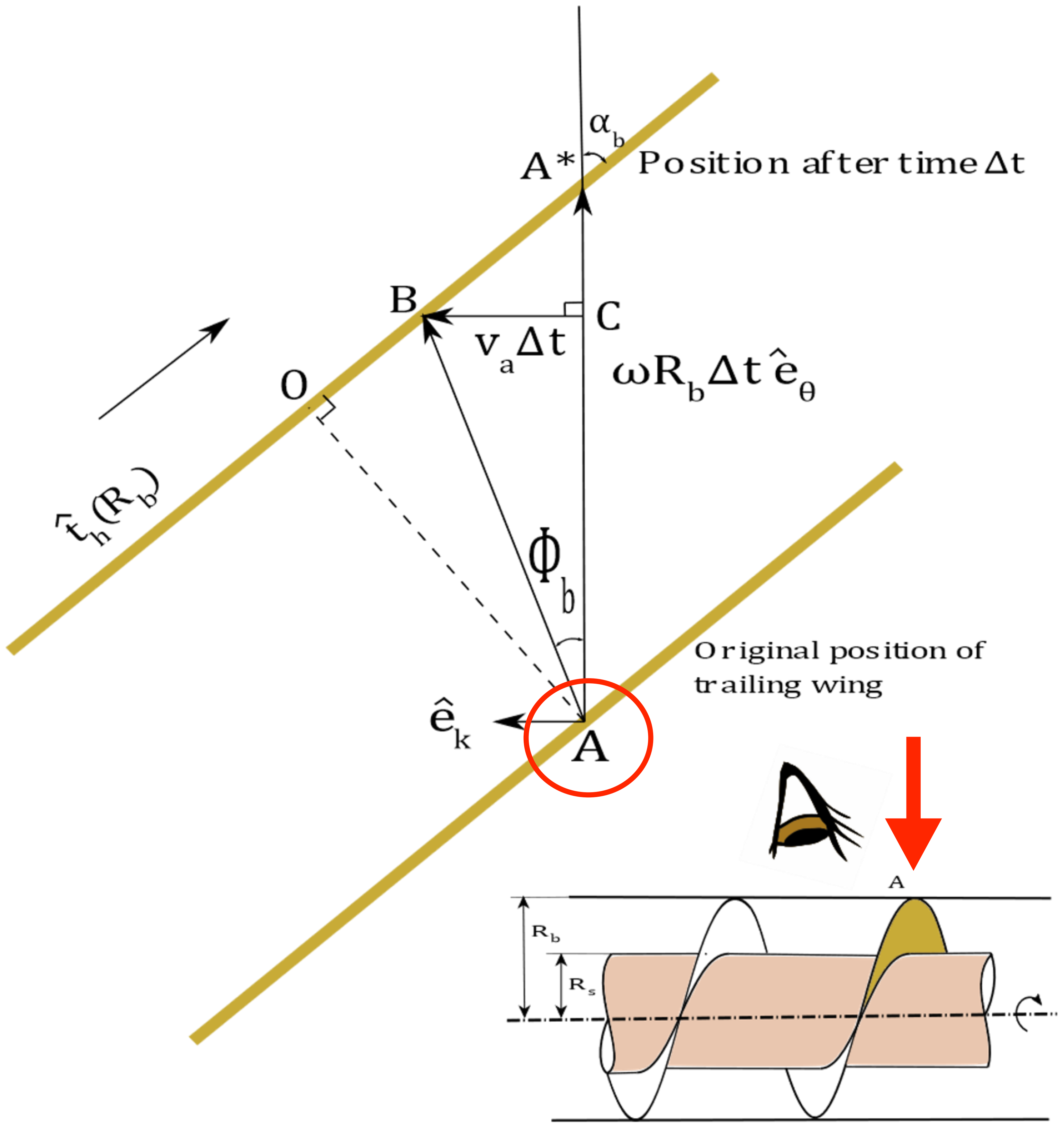

$$Q = \nu V_a \pi (R_b^2 - R_s^2)$$

$$\frac{V_a}{V_b} = \frac{BC}{AA^*} = \frac{BC}{AC + CA^*} = \frac{1}{\frac{1}{\tan\phi_b} + \frac{1}{\tan\alpha_b}}$$

$$V_a = V_b \frac{\tan\phi_b \tan\alpha_b}{\tan\alpha_b + \tan\phi_b}$$

$$V_b = \omega R_b$$

$$Q = \nu\, \omega R_b \frac{\tan\phi_b \tan\alpha_b}{\tan\alpha_b + \tan\phi_b}\, \pi \left(R_b^2 - R_s^2\right)$$

Wu, C. C. (1978), Masters thesis, Kansas State Univ.

Mechanics: forces on the sub-elements

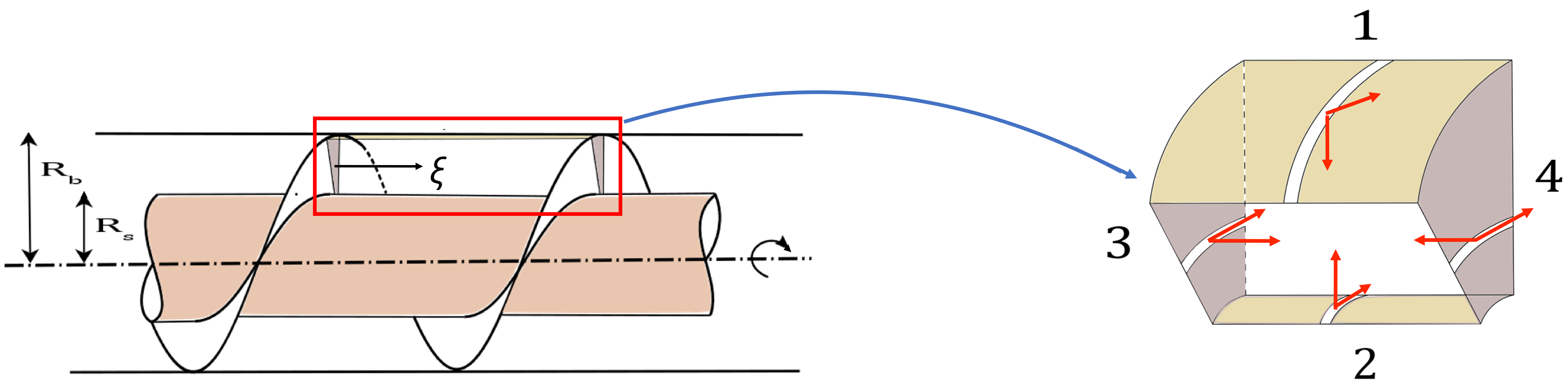

Force	Direction
$dF_{1n} = P_b(R_b d\theta d\xi)$	$-\hat{e}_r$
$dF_{1f} = \mu_b P_b(R_b d\theta d\xi)$	$-\cos\phi_b\,\hat{e}_\theta - \sin\phi_b\,\hat{e}_k$
$dF_{2n} = P_s(cR_b d\theta d\xi)$	$\hat{e}_r$
$dF_{2f} = \mu_s P_s(cR_b d\theta d\xi)$	$\hat{t}_h(R_s) = \cos\alpha_s\,\hat{e}_\theta - \sin\alpha_s\,\hat{e}_k$

Force	Direction
$dF_{3n} = P_{lw}\left(\left(\frac{rd\theta}{cos\alpha}\right)dr\right)$	$\hat{n}_h(r,\theta) = -\sin\alpha\,\hat{e}_\theta - \cos\alpha\,\hat{e}_k$
$dF_{3f} = \mu_w P_{lw}\left(\left(\frac{rd\theta}{cos\alpha}\right)dr\right)$	$\hat{t}_h(r) = \cos\alpha\,\hat{e}_\theta - \sin\alpha\,\hat{e}_k$
$dF_{4n} = P_{tw}\left(\left(\frac{rd\theta}{cos\alpha}\right)dr\right)$	$-\hat{n}_h(r,\theta) = \sin\alpha\,\hat{e}_\theta + \cos\alpha\,\hat{e}_k$
$dF_{4f} = \mu_w P_{tw}\left(\left(\frac{rd\theta}{cos\alpha}\right)dr\right)$	$\hat{t}_h(r) = \cos\alpha\,\hat{e}_\theta - \sin\alpha\,\hat{e}_k$

Linear Momentum Balances

Along $\hat{e}_r$

$$\boxed{c\overline{P_s(\xi)} - \overline{P_b(\xi)} + 2\overline{P} = 0}$$

Along $\hat{e}_\theta$

$$-\cos\phi_b\,\mu_b R_b \overline{P_b(\xi)} + c\mu_s R_b \overline{P_s(\xi)}\cos\alpha_s - \frac{p}{2\pi}\overline{P_{lw}(r)}$$
$$+\mu_w\left(\overline{rP_{lw}(r)}\right) + \frac{p}{2\pi}\overline{P_{tw}(r)} + \mu_w\left(\overline{rP_{tw}(r)}\right) = 0$$

Along $\hat{e}_k$

$$-\mu_b R_b \sin\phi_b\,\overline{P_b(\xi)} - \mu_s c R_b \sin\alpha_s \overline{P_s(\xi)} - \overline{rP_{lw}(r)}$$
$$-\frac{p\mu_w}{2\pi}\overline{P_{lw}(r)} + \overline{rP_{tw}(r)} - \frac{p\mu_w}{2\pi}\overline{P_{tw}(r)} = 0$$

$$\overline{\phi(x)} = \int_{x_i}^{x_f} \phi(x)\,dx$$

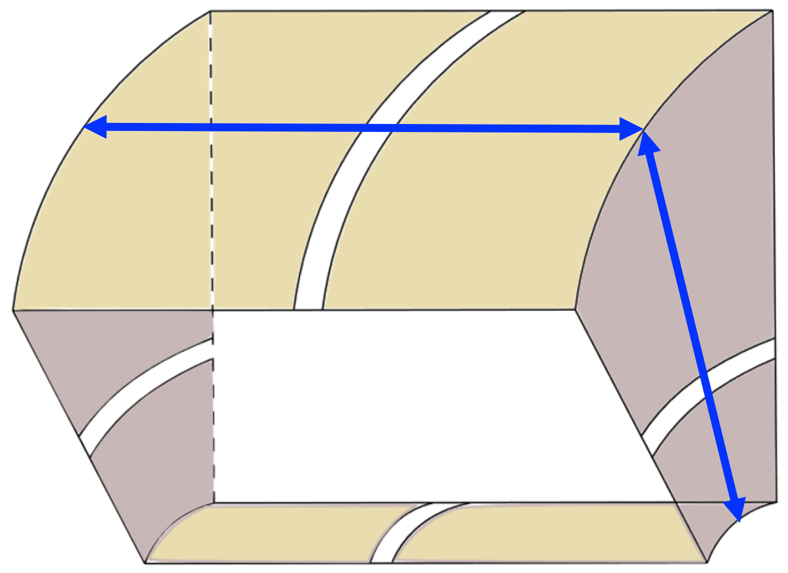

Angular Momentum Balances

All the moments are taken about a point on the axis of the shaft translated by $-\frac{p\theta}{2\pi}\hat{e}_k$ from the origin.

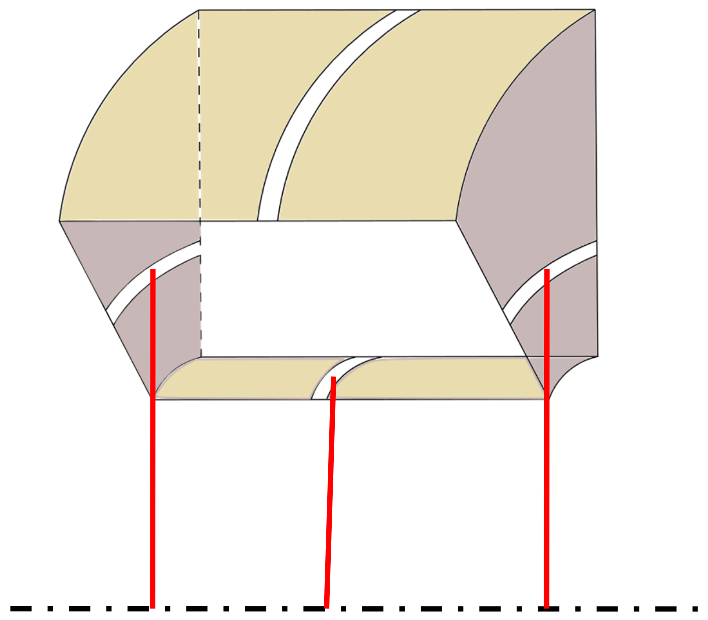

Along $\hat{e}_r$

$$-\cos\phi_b\mu_b R_b\overline{\xi P_b(\xi)} + \cos\alpha_s\mu_s c R_b\overline{\xi P_s(\xi)} + \frac{p^2}{2\pi}\overline{P_{tw}(r)} + p\mu_w\overline{rP_{tw}(r)} = 0$$

Along $\hat{e}_\theta$

$$R_b\overline{\xi P_b(\xi)} + R_b^2\sin\phi_b\mu_b\overline{P_b(\xi)} - cR_b\overline{\xi P_s(\xi)} + \sin\alpha_s\mu_s c^2 R_b^2\overline{P_s(\xi)}$$

$$+\overline{r^2 P_{lw}(r)} + \frac{p}{2\pi}\mu_w\overline{rP_{lw}(r)} - \overline{r^2 P_{tw}(r)} + \frac{p}{2\pi}\mu_w\overline{rP_{tw}(r)} = 0$$

Along $\hat{e}_k$

$$-R_b^2\cos\phi_b\mu_b\overline{P_b(\xi)} + \mu_s\cos\alpha_s c^2 R_b^2\overline{P_s(\xi)} - \frac{p}{2\pi}\overline{rP_{lw}(r)}$$

$$+\mu_w\overline{r^2 P_{lw}(r)} + \frac{p}{2\pi}\overline{rP_{tw}(r)} + \mu_w\overline{r^2 P_{tw}(r)} = 0$$

Number of unknowns and equations

More variables (11) than equations (6)!

- $\boxed{\phi_b}$
- $\overline{P(\xi, r)}$
- $\overline{P_s(\xi)}, \quad \overline{\xi P_s(\xi)}$
- $\overline{P_b(\xi)}, \quad \overline{\xi P_b(\xi)}$
- $\overline{P_{tw}(r)}, \quad \overline{r P_{tw}(r)}, \quad \overline{r^2 P_{tw}(r)}$
- $\overline{P_{lw}(r)}, \quad \overline{r P_{lw}(r)}, \quad \overline{r^2 P_{lw}(r)}$

Not surprising, as we do not have a constitutive relation for the stress.

However, we can get a solution when μ_s and $\mu_w = 0$

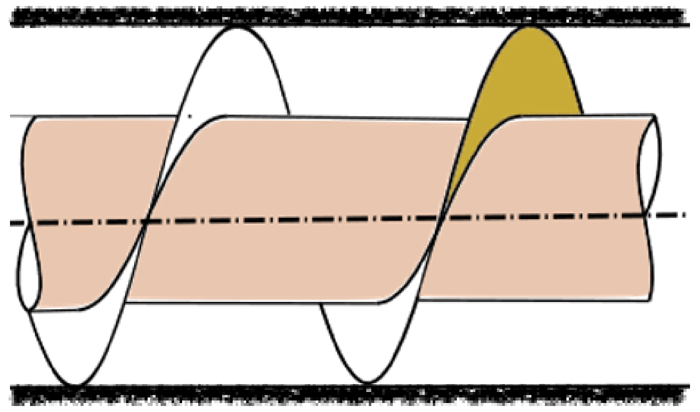

Screw and shaft surfaces frictionless

Linear momentum balance along $\hat{e}_k$ reduces to

$$-\mu_b R_b \sin\phi_b \overline{P_b(\xi)} - \overline{rP_{lw}}(r) + \overline{rP_{tw}(r)} = 0$$

Angular momentum balance along $\hat{e}_k$ reduces to

$$-R_b^2 \cos\phi_b \mu_b \overline{P_b(\xi)} - \frac{p}{2\pi}\overline{rP_{lw}(r)} + \frac{p}{2\pi}\overline{rP_{tw}(r)} = 0$$

Solving the above equations, we get:

$$\cot\phi_b = \frac{p}{2\pi R_b} = \tan\alpha_b$$

The expression for discharge rate simplifies to

$$Q = \nu\omega R_b \underbrace{\left[\frac{2\pi\,(p/R_b)}{(2\pi)^2 + (p/R_b)^2}\right]}_{f(p/R_b)} \pi(R_b^2 - R_s^2)$$

Dimensionless flow rate when μ_s and $\mu_w = 0$

$$Q = \nu\omega R_b f(p/R_b)\pi(R_b^2 - R_s^2)$$

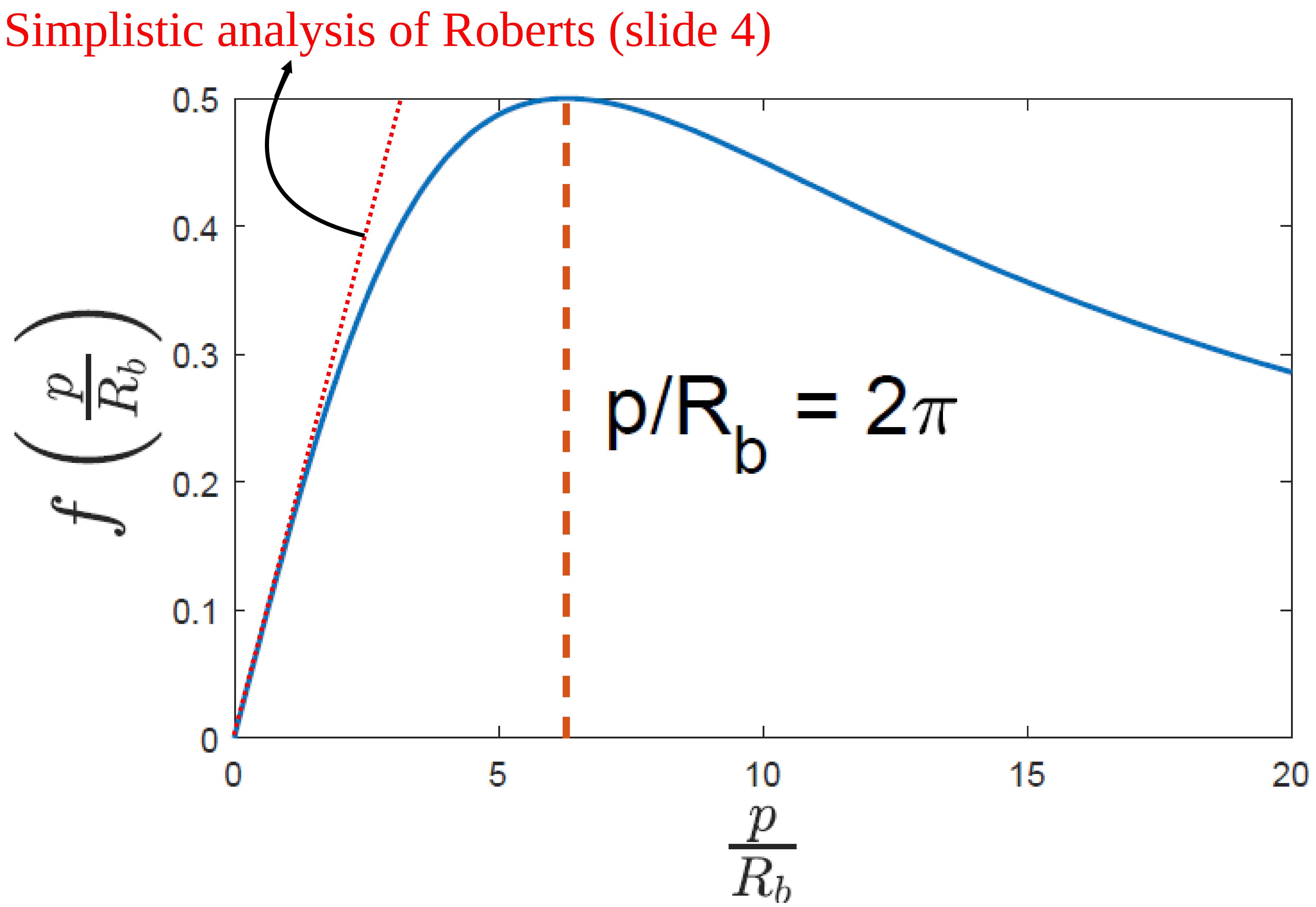

There is an optimum p/R_b at which discharge rate is maximum

DEM simulations of flow in a screw feeder

Verify predictions of simple model; relax simplifying assumptions; get details of the flow

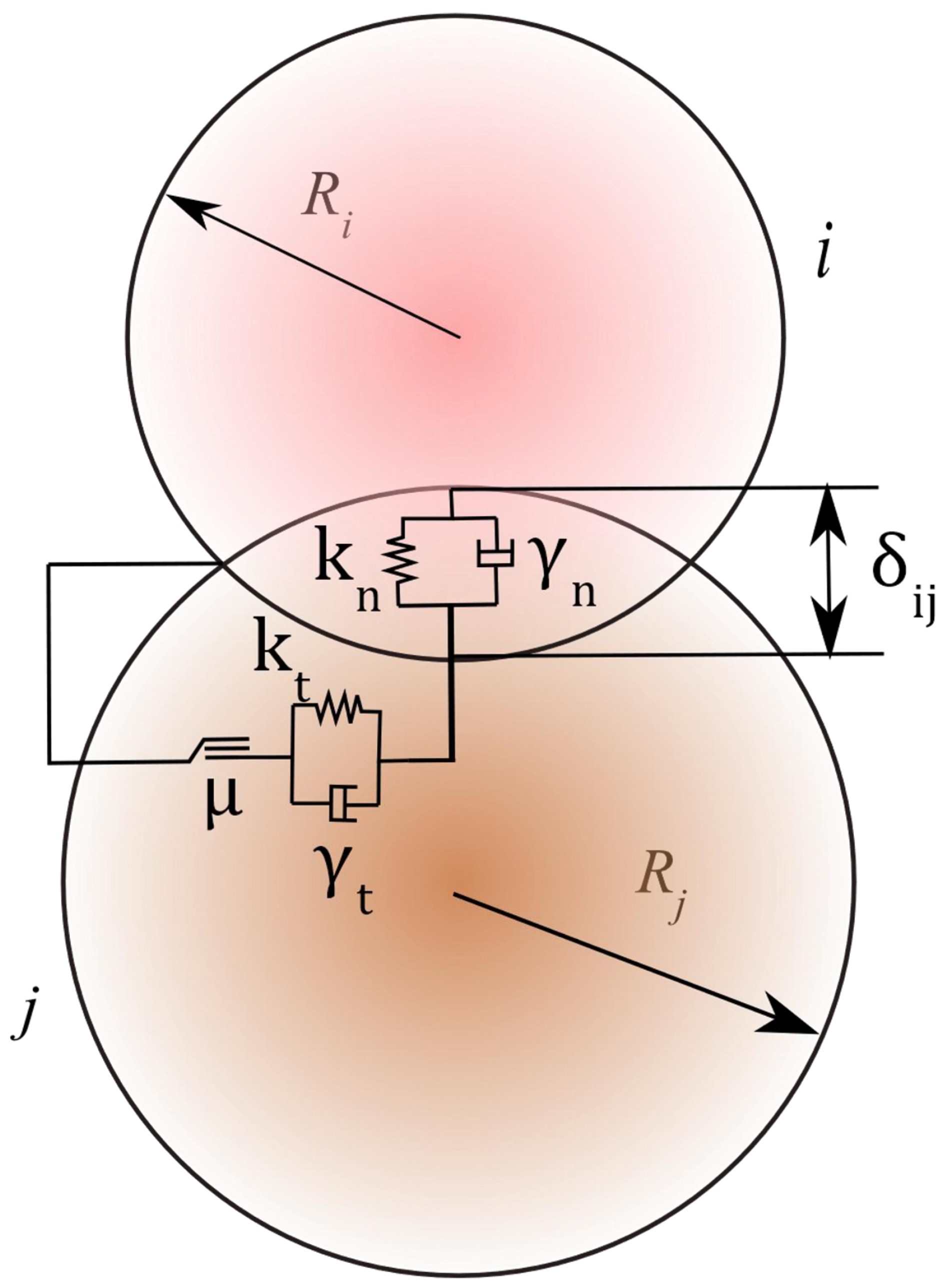

$$\mathbf{F}_n^{(i)} = k_n \delta \mathbf{n} - m_{eff} \gamma_n \mathbf{v}_n$$

$$\mathbf{F}_t^{(i)} = \begin{cases} -k_t \Delta \mathbf{s} - m_{eff} \gamma_t \mathbf{v}_t, & \left|\frac{\mathbf{F}_t}{\mathbf{F}_n}\right| < \mu \\ -\mu |\mathbf{F}_n^{(i)}| \frac{\mathbf{v}_t}{|\mathbf{v}_t|} & otherwise \end{cases}$$

$$m_i \frac{d\mathbf{v}_i}{dt} = m_i \mathbf{F}_i{}^b + \mathbf{F}_i{}^c$$

$$I_i \frac{d\omega_i}{dt} = \mathbf{T}_i{}^c$$

$$\mathbf{F}_i{}^c = \sum_{\substack{j=1 \\ j \neq i}}^{N} (\mathbf{F}_{ij}{}^n + \mathbf{F}_{ij}{}^t)$$

$$\mathbf{T}_i{}^c = \sum_{\substack{j=1 \\ j \neq i}}^{N} (R_i \mathbf{n}) \times (\mathbf{F}_{ij}{}^t)$$

Cundall, PA, & Strack, OD Geotechnique **29**, 47-65 (1979).

Simulation process overview

Carried out using the open source LIGGGHTS package

Geometric parameters in the DEM set-up

Geometric parameters	category I	category II
screw-shaft radius (R_s)	6.5 d_p	6.5 d_p
barrel radius (R_b)	19 d_p	(19 , 25.25, 31.5) d_p
pitch (p)	(38, 76, 114, 152, 190) d_p	38 d_p
blade thickness (t_b)	1 d_p	1 d_p

Creation of boundaries

Screw, shaft and casing surfaces created by triangulation

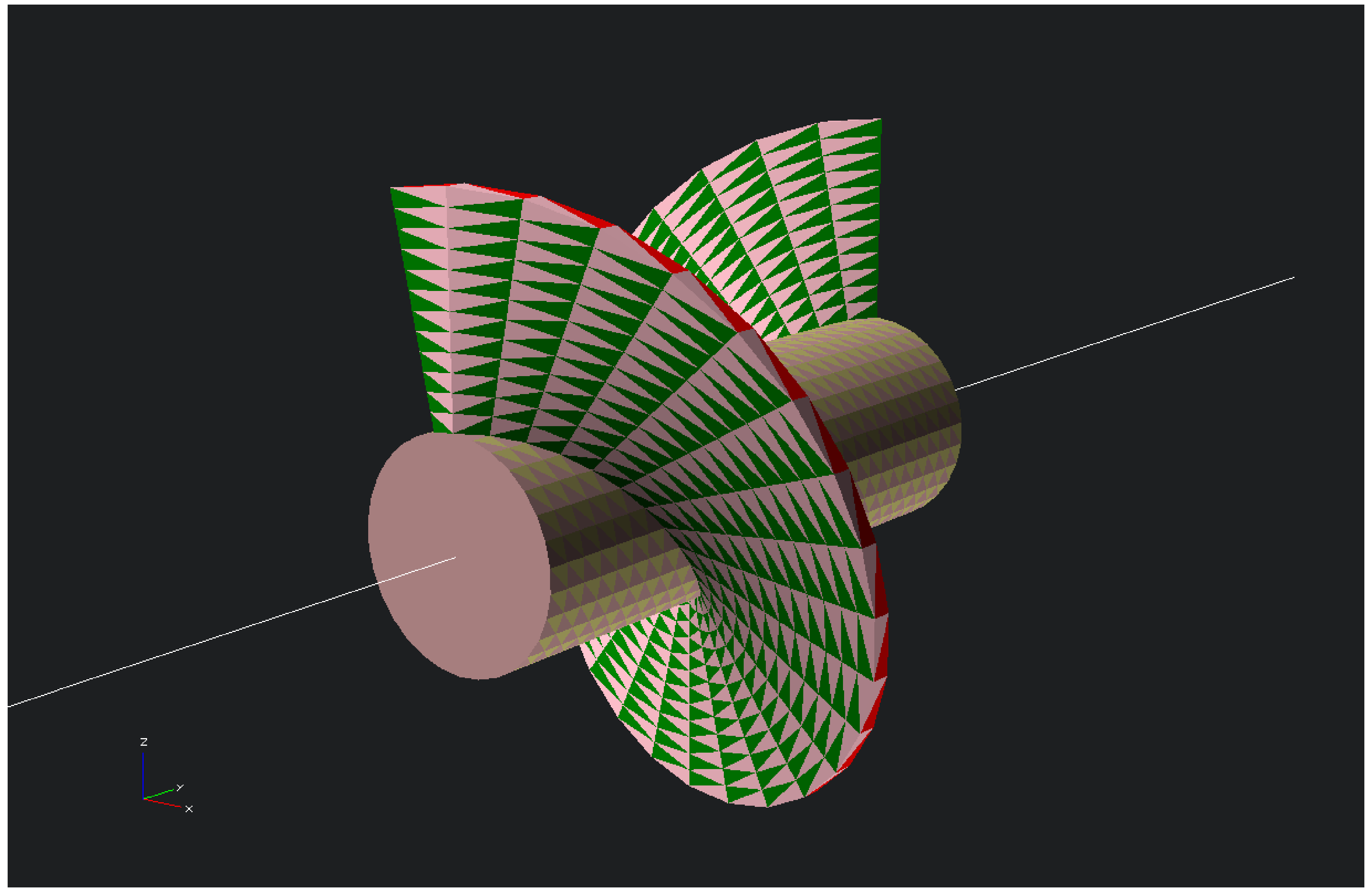

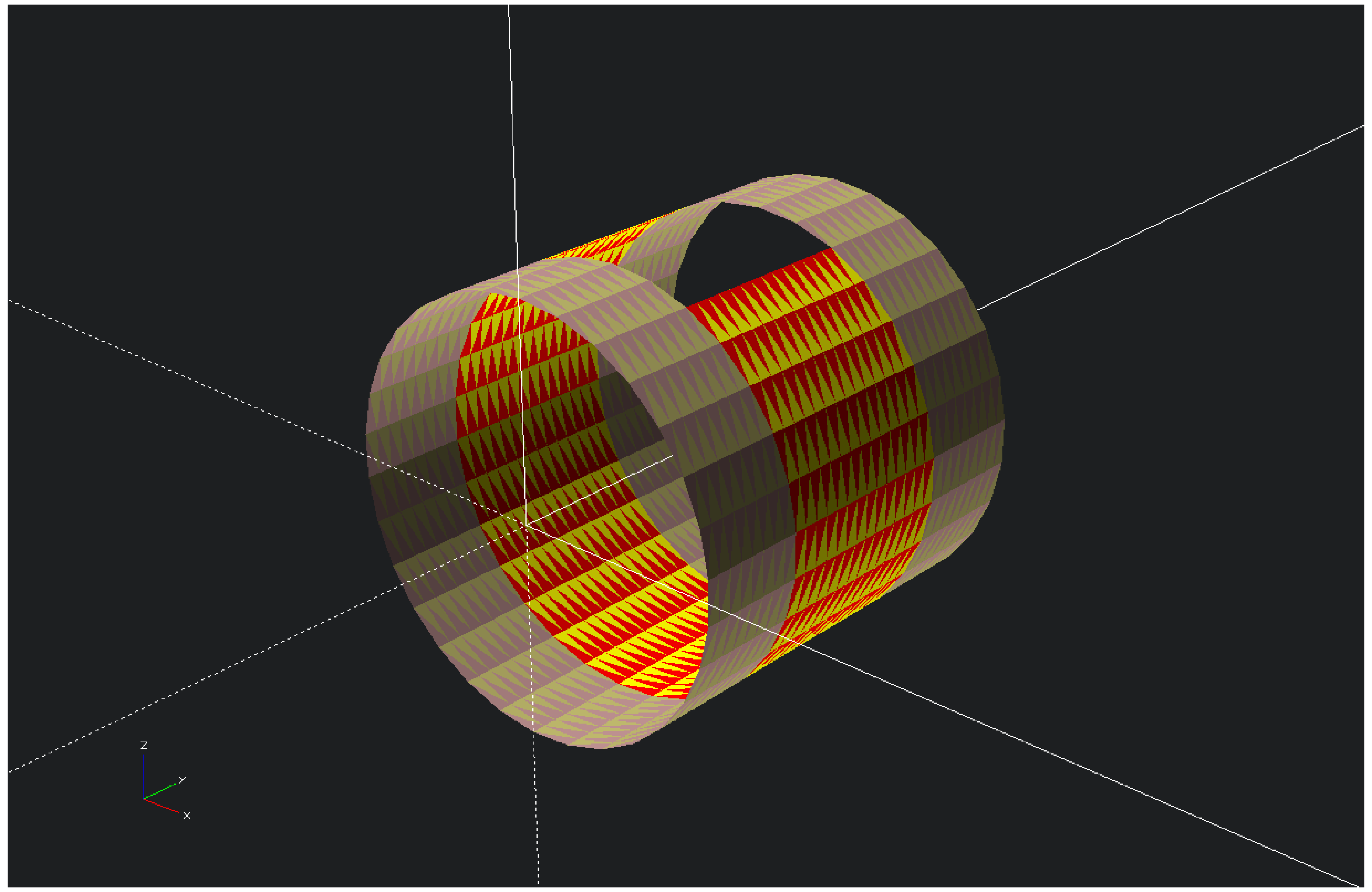

Averaging in the bulk and the surfaces

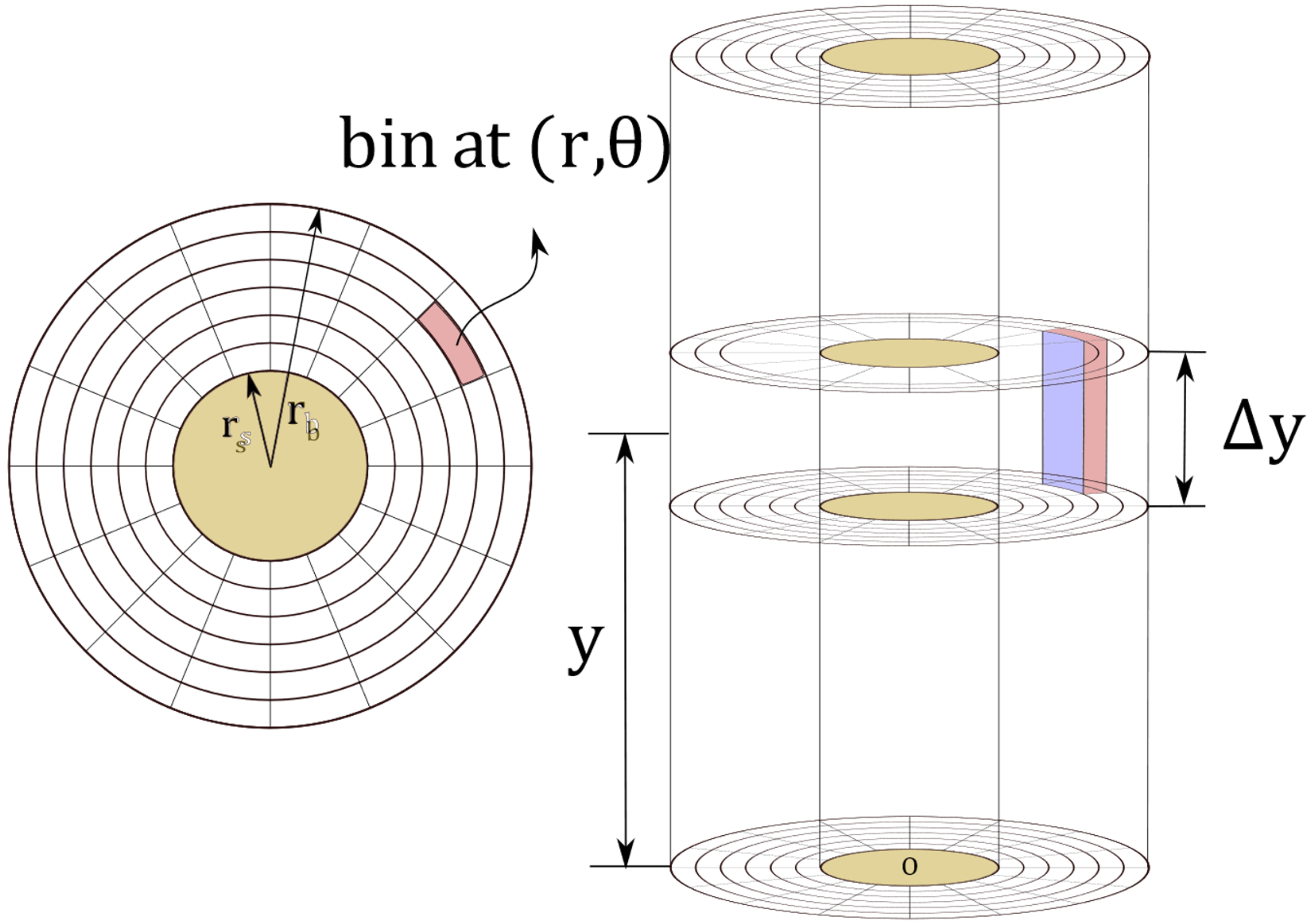

Annular ring
elements in the bulk

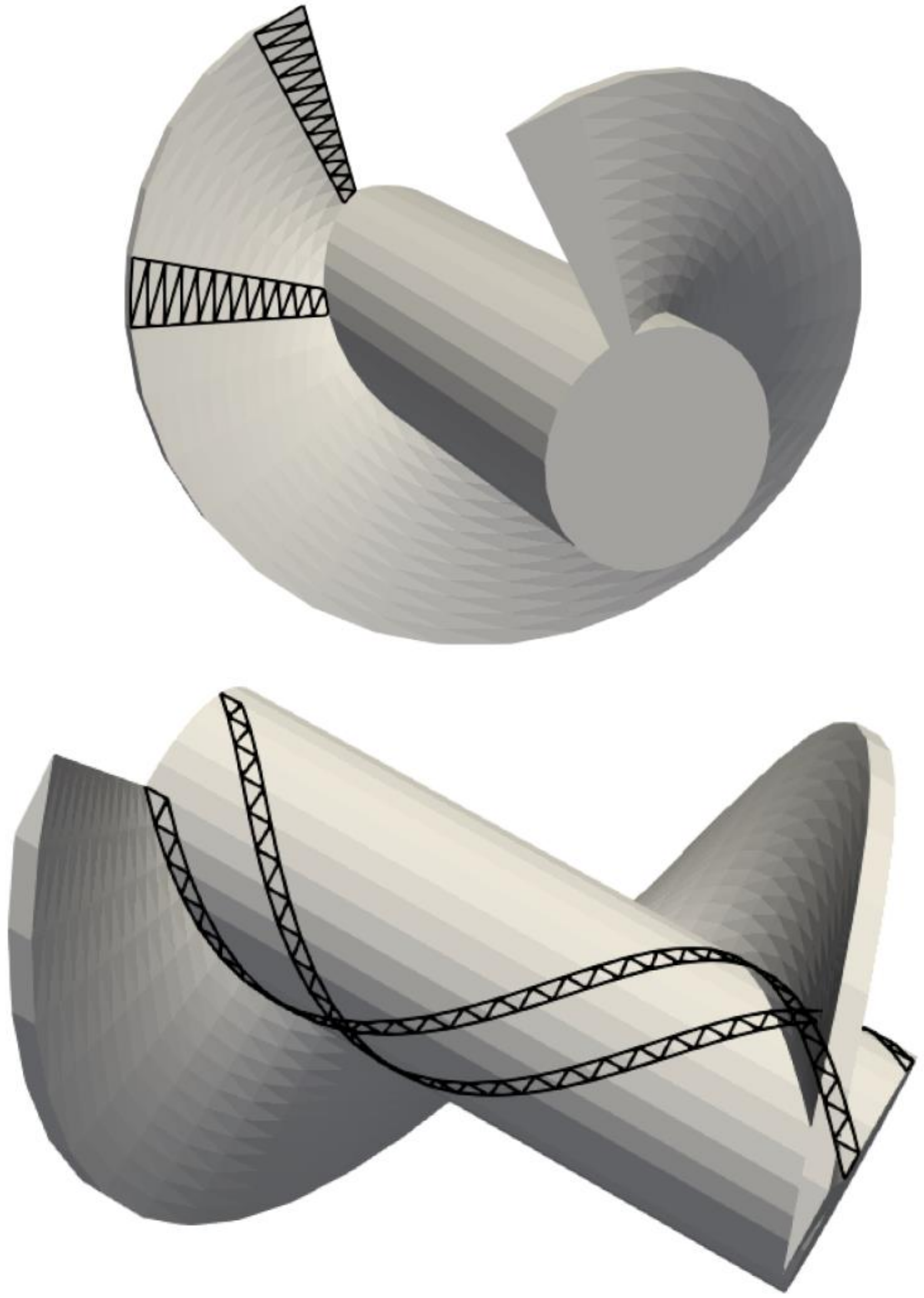

Triangular element
sets on the screw and
shaft surfaces

Variation of solid fraction and pressure in the bulk

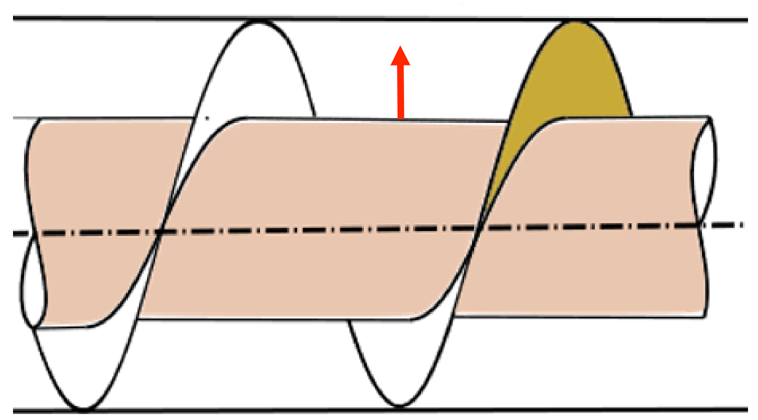

Solids fraction

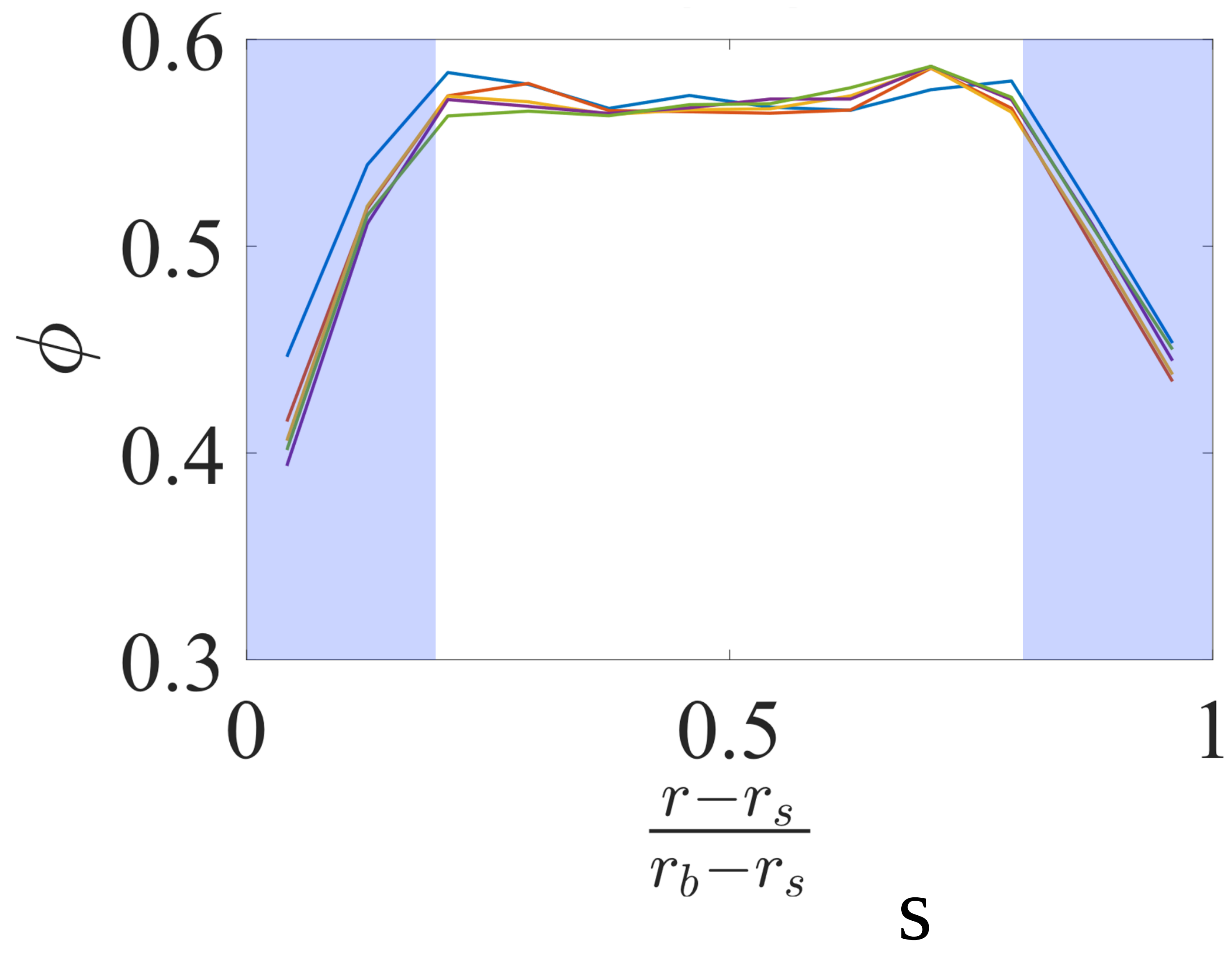

Pressure

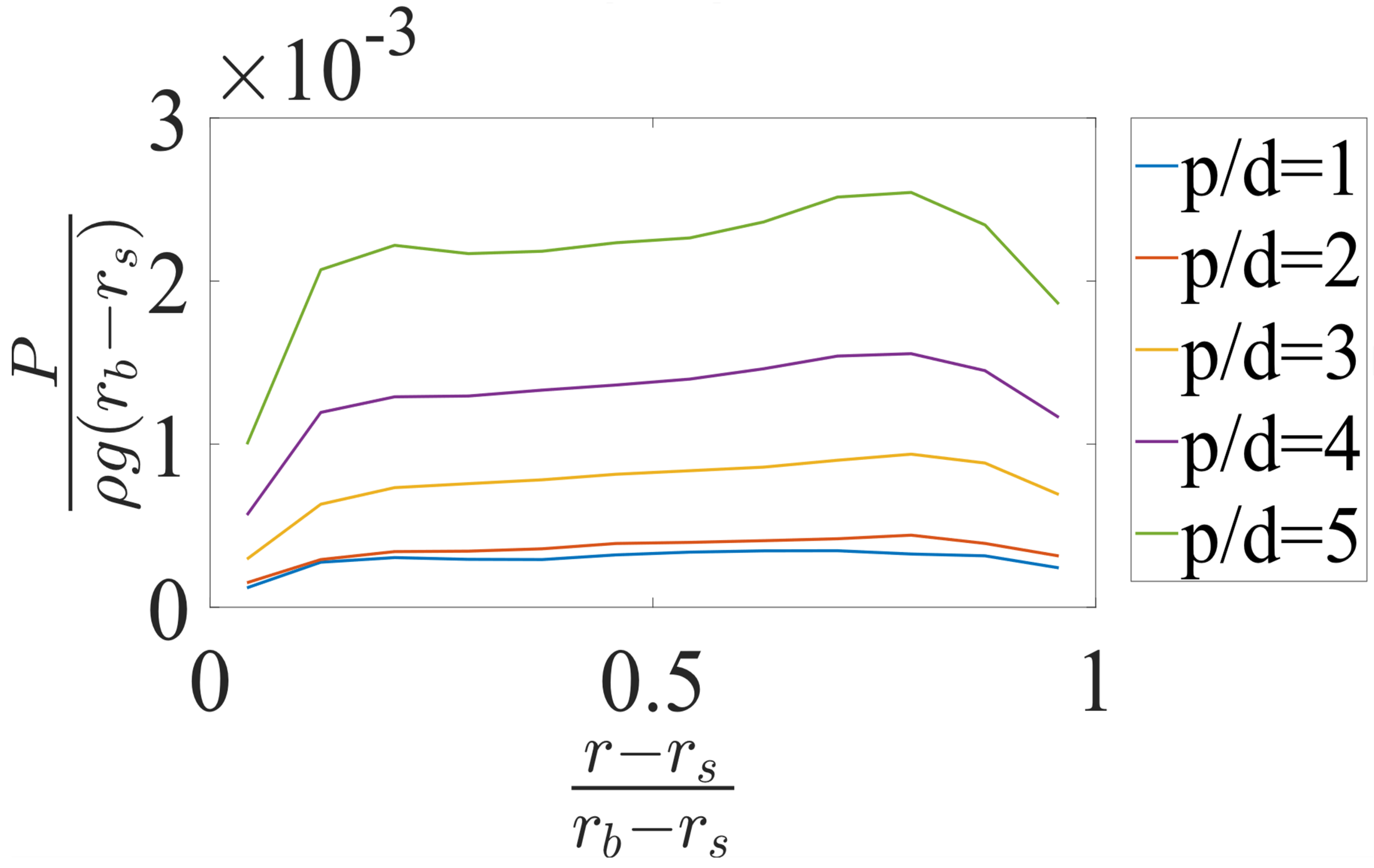

Lower solids fraction near the boundaries

Azimuthal and axial velocities

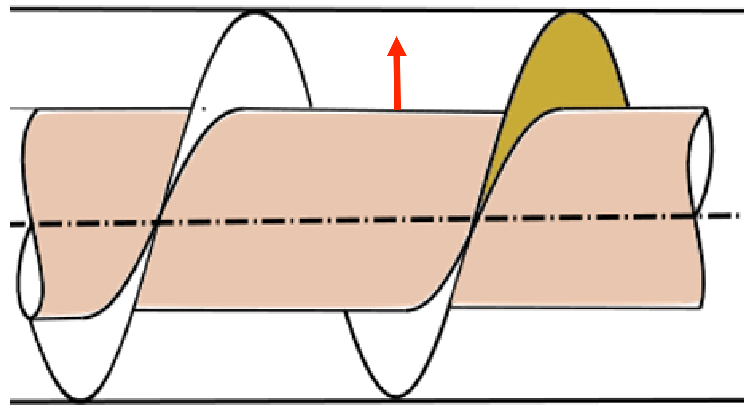

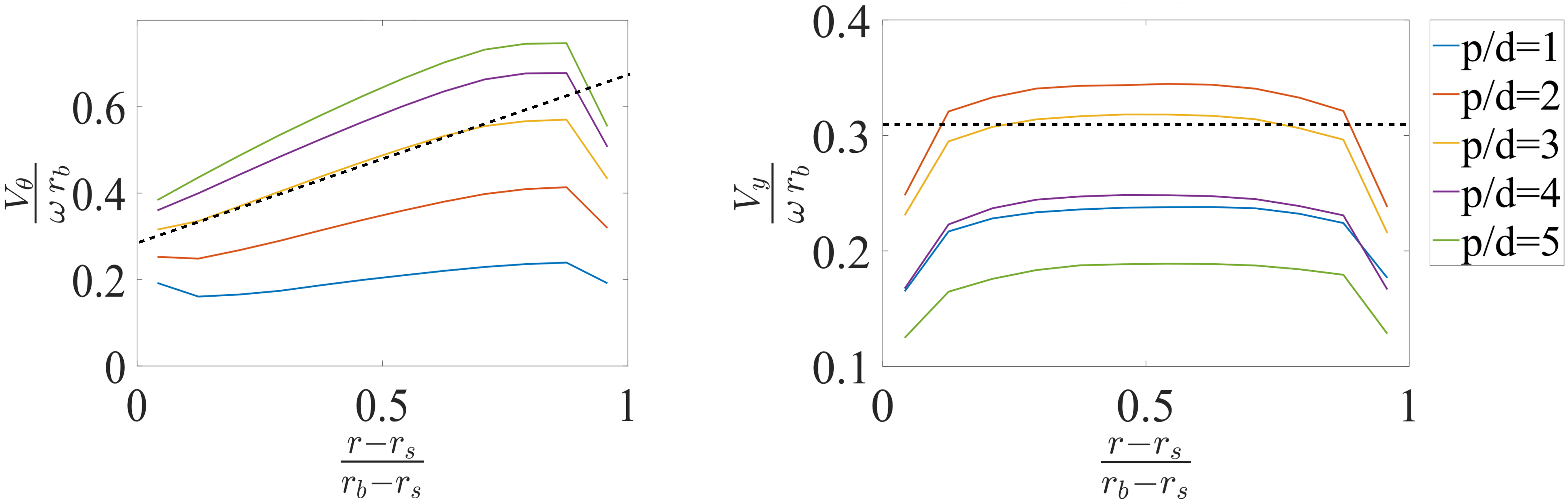

Motion nearly like that a rigid plug, except near the boundaries

Stresses on the barrel

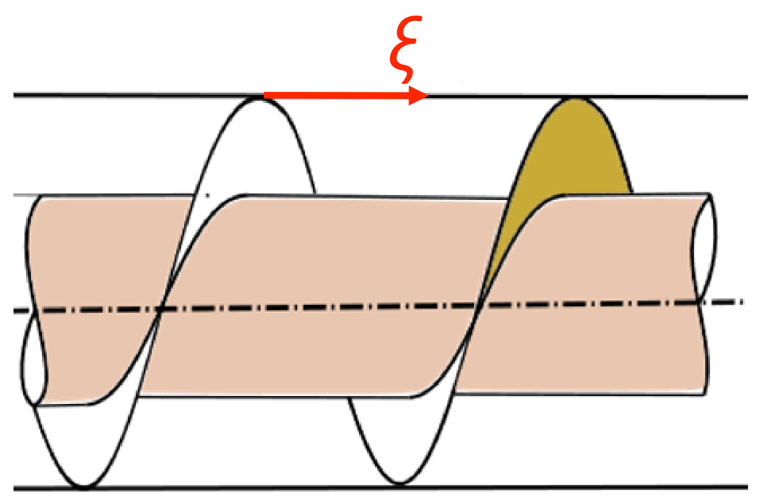

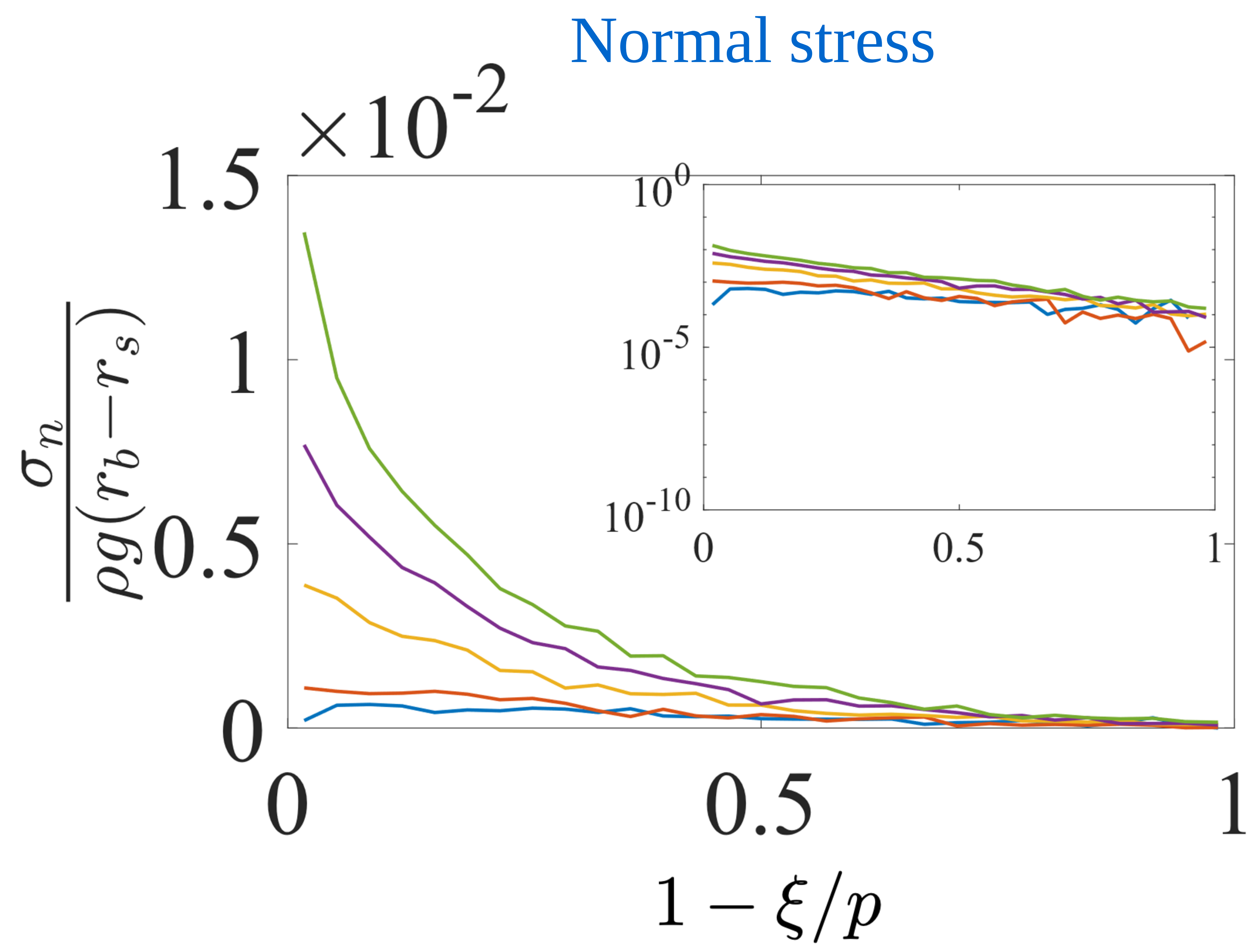

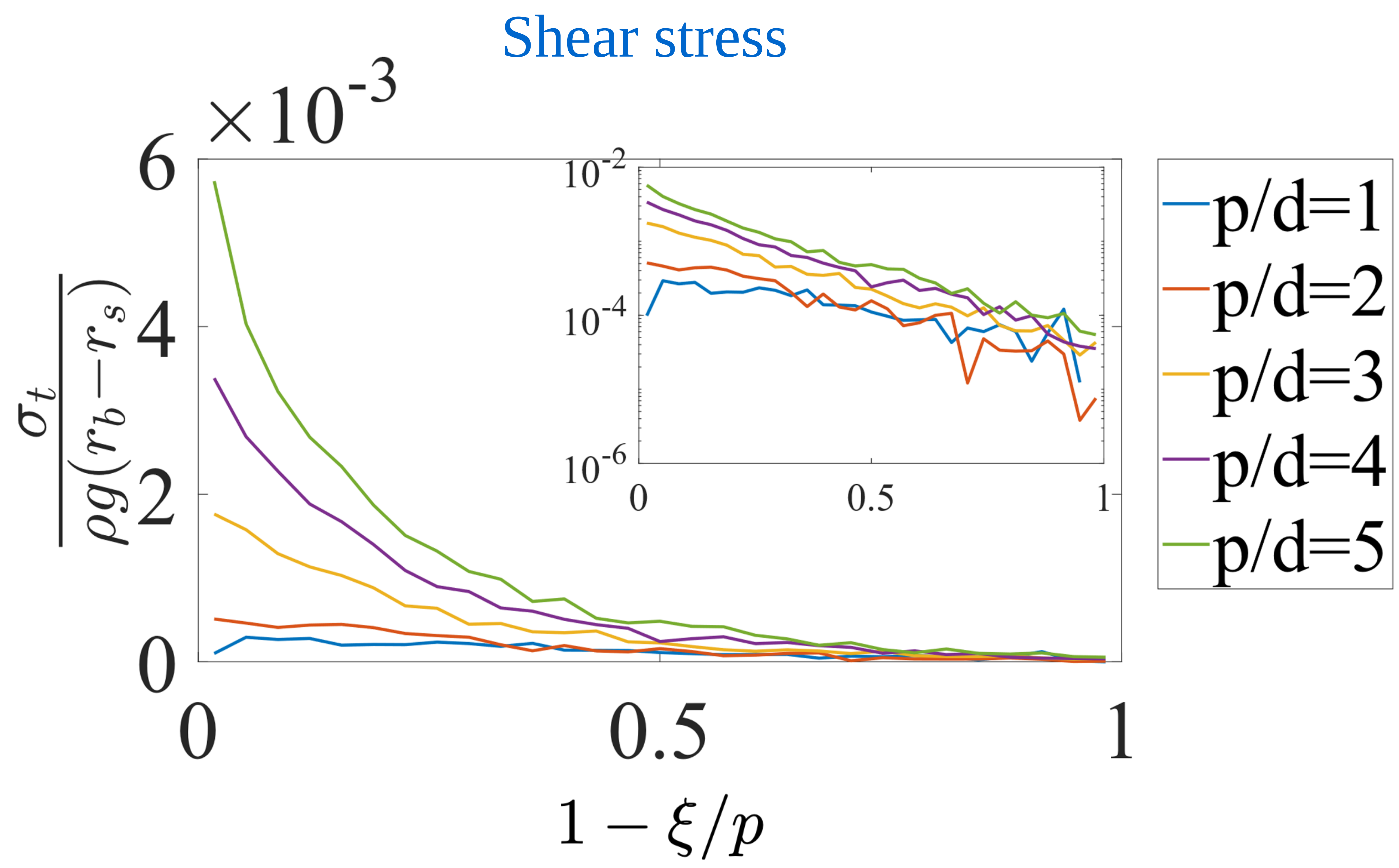

Exponential decay: similar to the Janssen saturation of stress in silos

Summary of the stress of surfaces in the absence of gravity

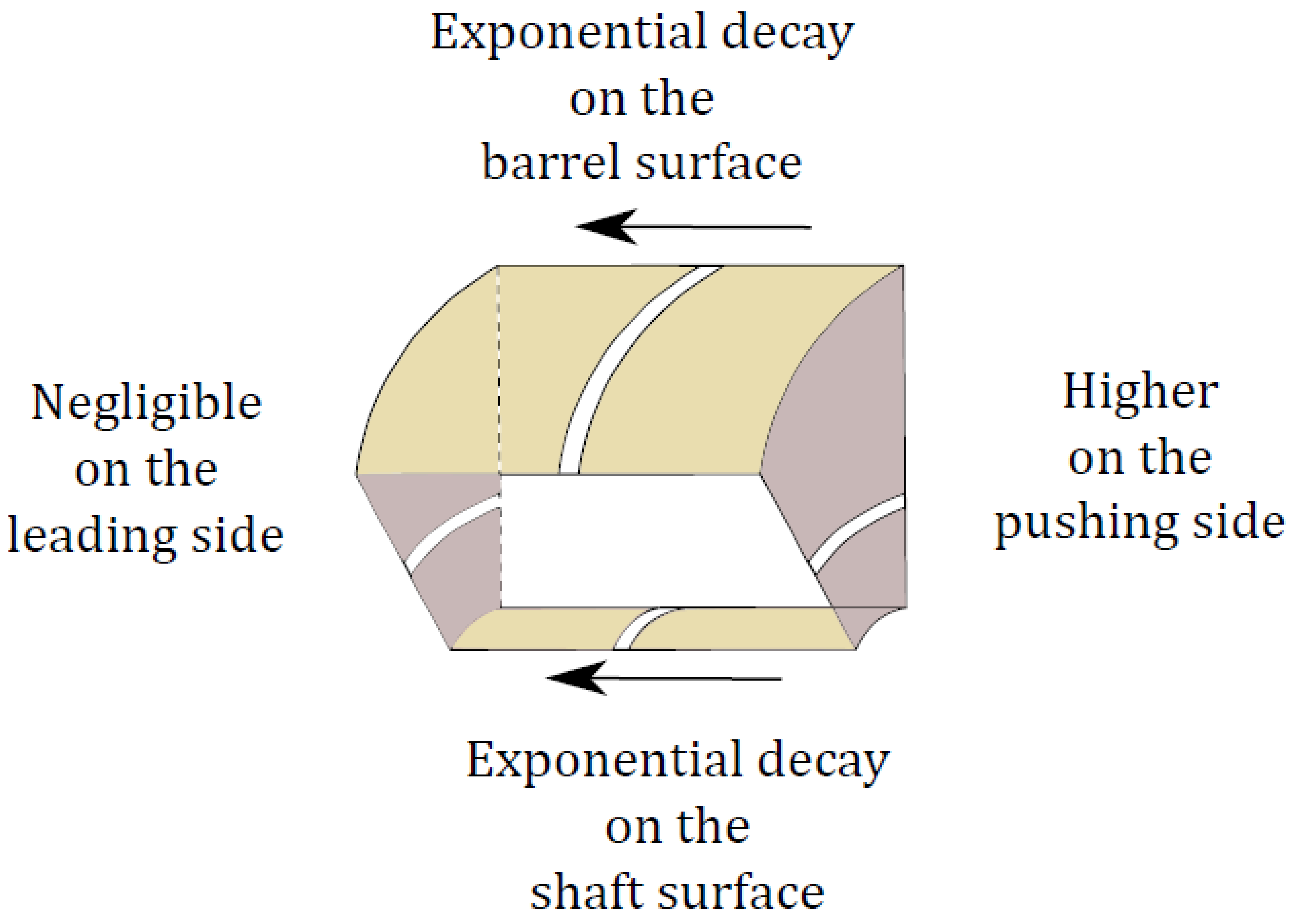

Results from DEM simulation under gravity

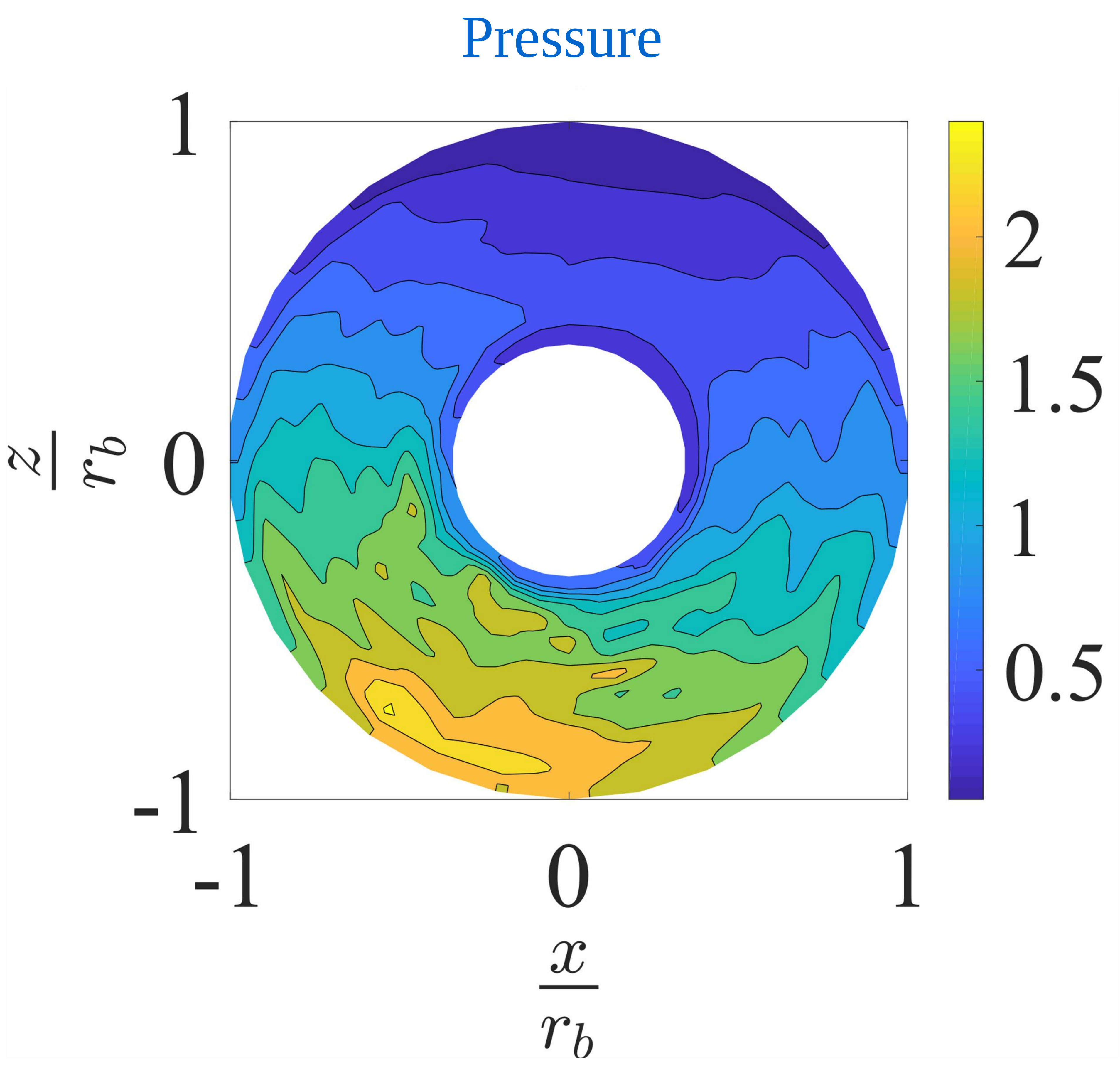

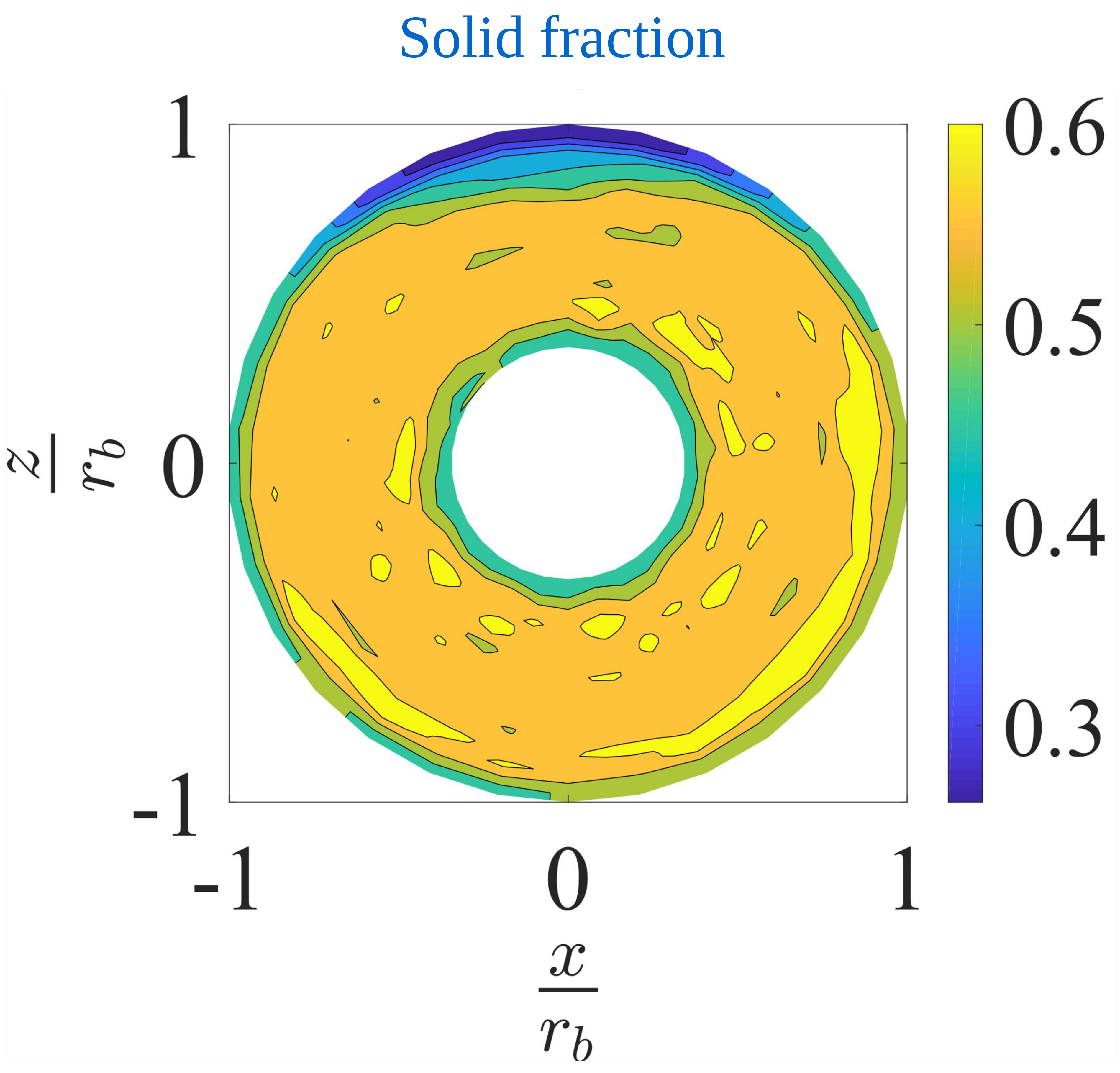

Results from simulations under gravity (Contd..)

Axial velocity

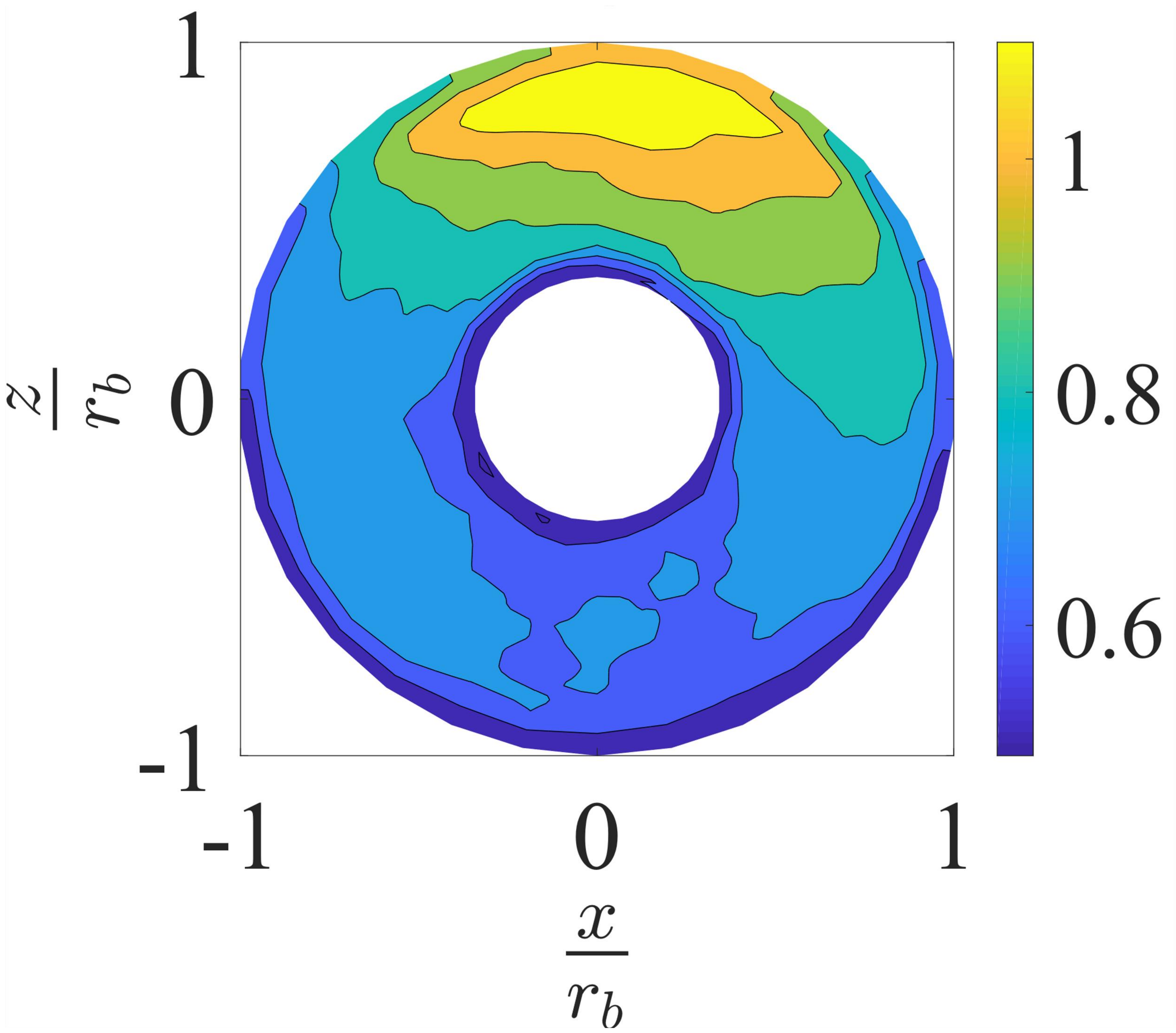

Azimuthal velocity

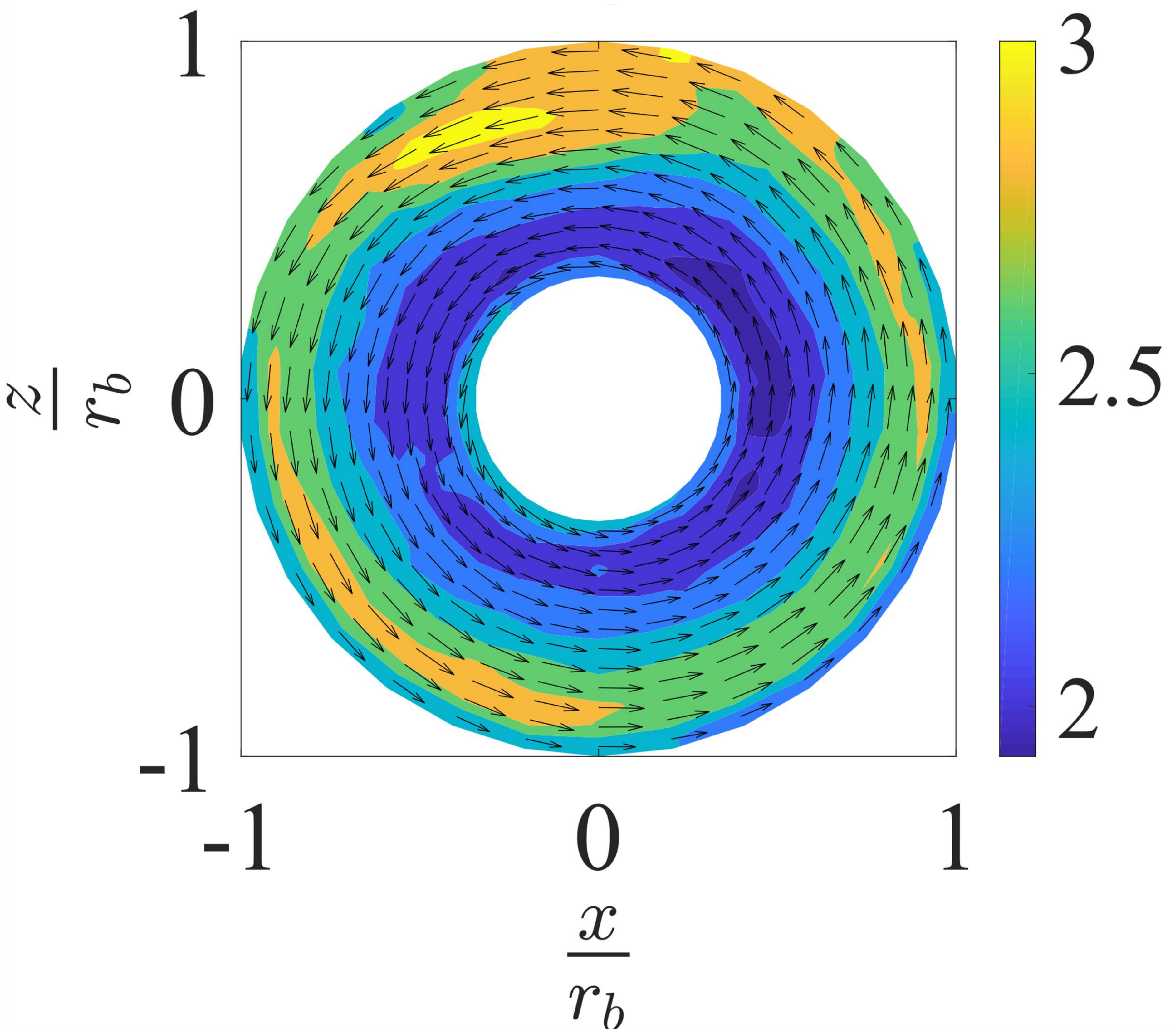

Comparison of DEM result with theory

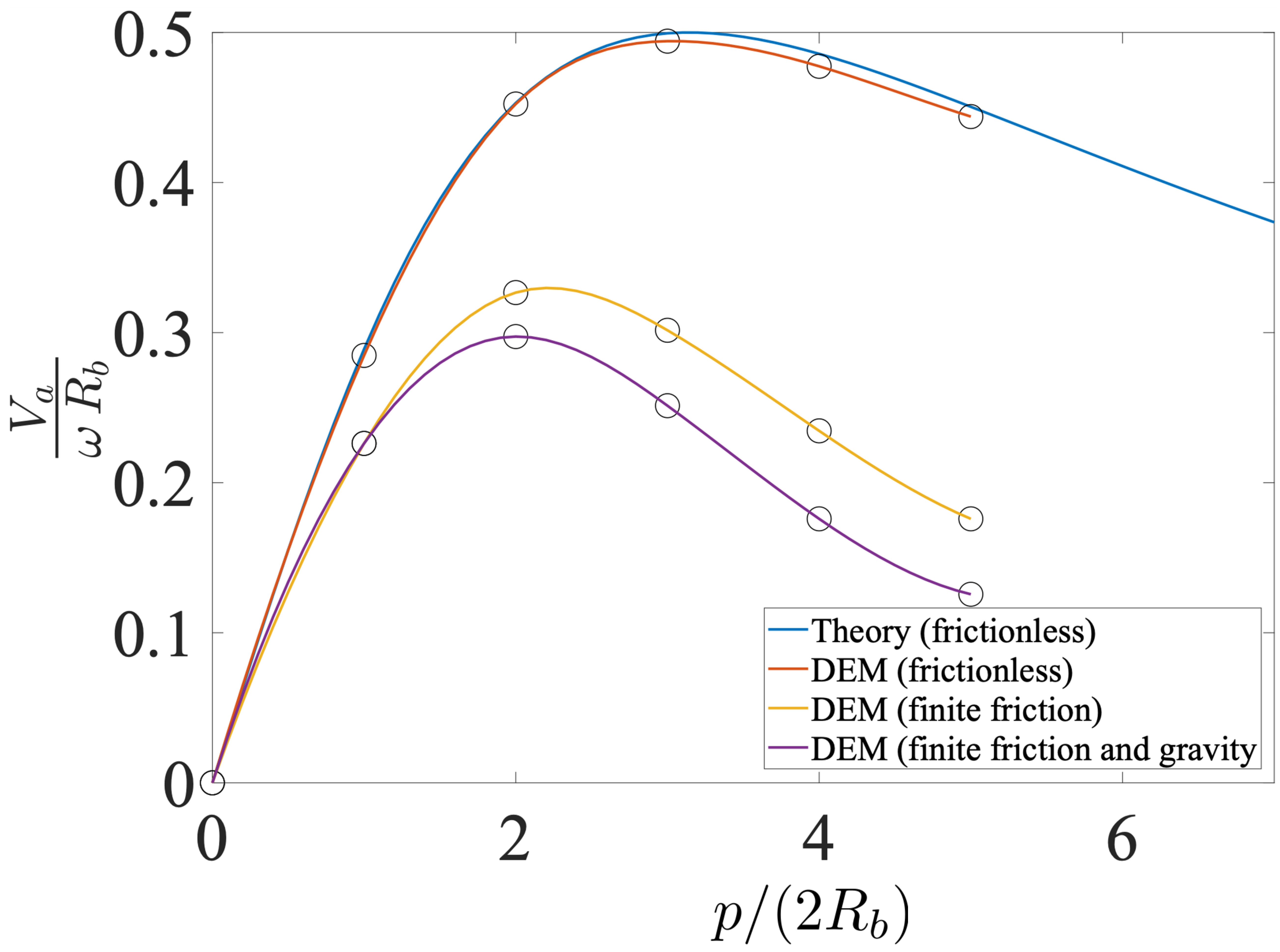

- Excellent agreement for frictionless screw surface
- Same qualitative trend for frictional surface, and when gravity is present
- There is always an optimum value of p/R_b at which discharge rate is maximum

Conclusion

- A mechanistic model for powder flow through a screw feeder developed.
- Balances of linear and angular momentum in the limit of vanishing friction coefficient on the screw surface solved to obtain maximum discharge rate.
- DEM simulations conducted to verify model predictions, relax assumptions, and provide insight. Excellent agreement with model predictions.
- The qualitative behavior of the average axial velocity curve doesn't change with the introduction of gravity.
- Ongoing and future work: experiments, extension to twin screw feeders, use more sophisticated models to determine density variation and discharge rate.